

Supporting Information

Supplemental material for “New insights in the mechanism of cation migration induced by cation-anion dynamic coupling in superionic conductors”

Siyuan Wu, Ruijuan Xiao, Hong Li*, Liquan Chen*

Bond-valence results:

Here we show the details of Figure 1(a) in the Table S1 and we can conclude that the larger ratio between E_{mig} and E_{rots} , the more rotational-mode contribute to the coupling.

Table S1. The results of BV as shown in Figure 1(a) for compounds reported in Refs. 18-39

Chemical formula	ICSD id	E_{rots} [eV]	E_{mig} [eV]	E_{mig}/E_{rots}	Main coupling mode
Li ₂ SO ₄	icsd_201117	0.1	3.79	37.90	rotate
Li ₂ SO ₄	icsd_030276	0.39	2.93	7.51	rotate
Li ₂ SO ₄	icsd_153807	0.46	0.56	1.22	vibrate
Na ₂ SO ₄	icsd_062516	0.21	3.12	14.86	rotate
Na ₂ SO ₄	icsd_027654	0.29	1.7	5.86	rotate
Na ₂ SO ₄	icsd_066554	0.29	2.39	8.24	rotate
Na ₂ SO ₄	icsd_081504	0.26	2.94	11.31	rotate
Li ₃ WO ₄	icsd_067236	0.3	0.54	1.80	vibrate
Na ₃ WO ₄	icsd_028474	0.62	0.62	1.00	vibrate
K ₄ N ₂ O ₅	icsd_036640	0.49	4.01	8.18	rotate
Na ₃ ONO ₂	icsd_001352	0.41	1.74	4.24	rotate
Na ₃ ONO ₂	icsd_050768	0.3	2.59	8.63	rotate
NaNO ₃	icsd_031011	0.05	3.23	64.60	rotate
Na ₂ CO ₃	icsd_081004	0.21	3.26	15.52	rotate
Na ₂ CO ₃	icsd_080996	0.23	3.44	14.96	rotate
Na ₂ CO ₃	icsd_168129	0.5	2.66	5.32	rotate
Na ₂ SiF ₆	icsd_016598	0.08	0.78	9.75	rotate
Na ₂ SiF ₆	icsd_030348	0.07	0.85	12.14	rotate
Na ₃ AlF ₆	icsd_074210	0.07	0.97	13.86	rotate

Na ₃ AlF ₆	icsd_164685	0.07	0.99	14.14	rotate
Li ₃ PO ₄	icsd_010257	0.48	1.26	2.63	rotate
Li ₃ PO ₄	icsd_020208	0.49	0.95	1.94	vibrate
Na ₃ PO ₄	icsd_014090	0.62	6.93	11.18	rotate
Na ₃ PO ₄	icsd_033719	0.63	4.29	6.81	rotate
Li ₃ PS ₄	icsd_035018	1.18	1.22	1.03	vibrate
Li ₃ PS ₄	icsd_180318	0.66	0.79	1.20	vibrate
Li ₆ PS ₅ Cl	icsd_418488	1.06	2.78	2.62	rotate
Li ₆ PS ₅ Br	icsd_418490	0.63	2.96	4.70	rotate
Li ₆ PS ₅ I	icsd_421083	0.64	3.2	5.00	rotate
Li ₆ PS ₅ I	icsd_418489	0.49	3.03	6.18	rotate
Na ₁₁ Sn ₂ PS ₁₂		0.64	4.2	6.56	rotate
Na ₃ SbS ₄	icsd_044707	1.07	1.07	1.00	vibrate
Na ₁₁ Sn ₂ SbS ₁₂		1.02	2.8	2.75	rotate
LiBH ₄	icsd_168802	0.68	2.15	3.16	rotate
LiBH ₄	icsd_173101	0.11	1.41	12.82	rotate
LiBH ₄	icsd_173103	0.33	1.12	3.39	rotate
LiBH ₄	icsd_180103	0.57	2.38	4.18	rotate
Na ₃ YCl ₆	icsd_2057626	0.12	0.46	3.83	rotate
Na ₂ ZrCl ₆	icsd_2057627	0.33	1.05	3.18	rotate
Li ₂ BF ₅	icsd_426821	0.08	0.61	7.63	rotate
LiBF ₄	icsd_171375	0.09	1.03	11.44	rotate

Li₃PO₄:

Here we compare the two isomers of Li₃PO₄ (icsd_010257 and icsd_020208) and find that E_{rot} of O²⁻ anions are the same for two structures (about 0.50eV) while E_{mig} are different.

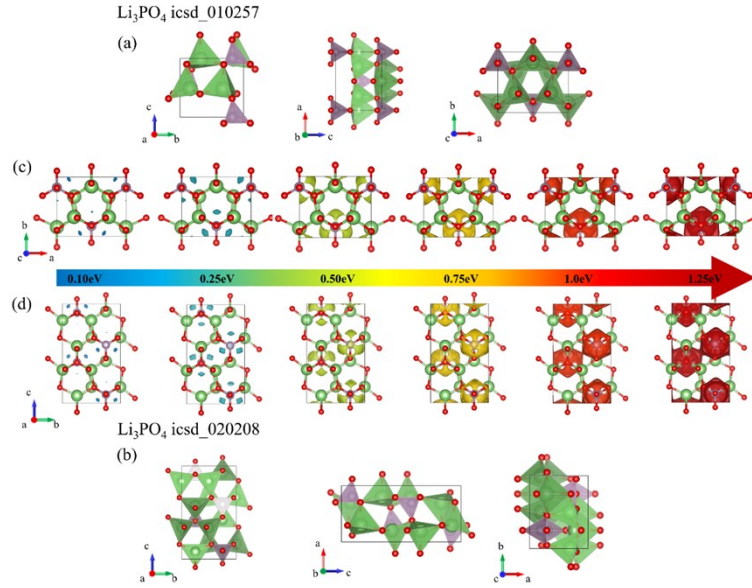


Figure S1. (a) and (b) are the top view of icsd_010257 and icsd_020208 from *a*, *b* and *c* axis respectively. The potential energy isosurfaces of the O²⁻ anions for Li₃PO₄ in (c) icsd_010257 and (d) icsd_020208 at 0.10eV, 0.25eV, 0.50eV, 0.75eV, 1.00eV and 1.25eV.

Simple harmonic vibration:

First, we consider without extra vibration. If the vibration equation is written as Equation S1, the maximum displacement is the amplitude *A* which represents the maximum excursion for ion. In the following the change of the *A* is discussed and used as the indicator for the ability of ion migration.

$$x = A \cos(\omega t + \varphi) \quad (\text{S1})$$

Then we consider the case where anion vibration direction is perpendicular to that of the migration direction of cation. The vibration equation of cation and anion can be written in Equation S2 and S3 respectively, the complex vibration of cation can be written as Equation S4. The Equation S4 is a function of *hyperbola* and can be written in the standard form (Equation S5) if we suppose *A_c* is larger than *A_a* (vice versa). When the frequencies for cation and anion are not the same the complex

vibration forms as *Lissajous* Figures and the effect on the cation migration is hard to predict. Fortunately, the truth in most cases in superionic materials is the two frequencies are subequal or at least in the similar orders of magnitude. When the frequencies are the same, Equation S6 is obtained as a function of *ellipse* and will degenerate into the *circle* or the line segment otherwise it forms a series of *Lissajous* Figures. So it can enhance the amplitude of cation as expressed in Equation S7, but also change the direction of cation and the same for the different frequencies.

$$x_c = A_c \cos(\omega_c t + \varphi_c) \quad (S2)$$

$$y_a = A_a \cos(\omega_a t + \varphi_a) \quad (S3)$$

$$\frac{x_c^2}{A_c^2} + \frac{y_a^2}{A_a^2} - \frac{2x_c y_a}{A_c A_a} \cos[(\omega_c - \omega_a)t + (\varphi_c - \varphi_a)] = \sin^2[(\omega_c - \omega_a)t + (\varphi_c - \varphi_a)]$$

$$\frac{x_c^2}{(A_c^2 + A_a^2) + \sqrt{(A_c^2 - A_a^2)^2 + 4A_c A_a \cos^2[(\omega_c - \omega_a)t + (\varphi_c - \varphi_a)]}} + \quad (S4)$$

$$\frac{y_a^2}{(A_c^2 + A_a^2) - \sqrt{(A_c^2 - A_a^2)^2 + 4A_c A_a \cos^2[(\omega_c - \omega_a)t + (\varphi_c - \varphi_a)]}} = 1 \quad (S5)$$

$$\frac{x_c^2}{(A_c^2 + A_a^2) + \sqrt{(A_c^2 - A_a^2)^2 + 4A_c A_a \cos^2(\varphi_c - \varphi_a)}} + \frac{y_a^2}{(A_c^2 + A_a^2) - \sqrt{(A_c^2 - A_a^2)^2 + 4A_c A_a \cos^2(\varphi_c - \varphi_a)}} = 1 \quad (S6)$$

$$A'_c = \sqrt{\frac{(A_c^2 + A_a^2) + \sqrt{(A_c^2 - A_a^2)^2 + 4A_c A_a \cos^2(\varphi_c - \varphi_a)}}{2}} \quad (S7)$$

Then we consider the case where anion vibration direction is parallel to that of the migration direction of cation and suppose the alone vibration equation of cation and anion can be written as Equation S8 and S9. The amplitude of cation is deduced as Equation S11. It will always enhance the vibration of cation when $A_a > 2A_c$ otherwise it should satisfy Equation S12 when the frequencies are the same while it should satisfy the Equation S13 when the frequencies are the different. The Δt in

Equation S13 represents time interval between two diffusion events. So we can infer that the close frequencies benefit the diffusion of Li^+ . Here we must emphasize if A_a is too large, the change of the PES will be large and it may turn into the rotation-coupling mode which will be discussed later.

$$x_c = A_c \cos(\omega_c t + \varphi_c) \quad (\text{S8})$$

$$x_a = A_a \cos(\omega_a t + \varphi_a) \quad (\text{S9})$$

$$x = \sqrt{A_c^2 + A_a^2 + 2A_c A_a \cos[(\omega_c - \omega_a)t + (\varphi_c - \varphi_a)]} \cos\left(\frac{\omega_c + \omega_a}{2}t + \frac{\varphi_c + \varphi_a}{2} - \varphi\right) \quad (\text{S10})$$

$$A'_c = \sqrt{A_c^2 + A_a^2 + 2A_c A_a \cos[(\omega_c - \omega_a)t + (\varphi_c - \varphi_a)]} \quad (\text{S11})$$

$$|\varphi_c - \varphi_a| < \arccos\left(-\frac{A_a}{2A_c}\right) \quad (\text{S12})$$

$$\Delta t < \frac{2 \arccos\left(-\frac{A_a}{2A_c}\right)}{|\omega_c - \omega_a|} \quad (\text{S13})$$

AIMD results:

The displacements in AIMD for LiBF_4 and Li_2BF_5 are shown in Figure S2(a) and (b) respectively. Figure S2(c) and (d)-(g) are the trajectories of Li^+ ions in LiBF_4 and Li_2BF_5 respectively.

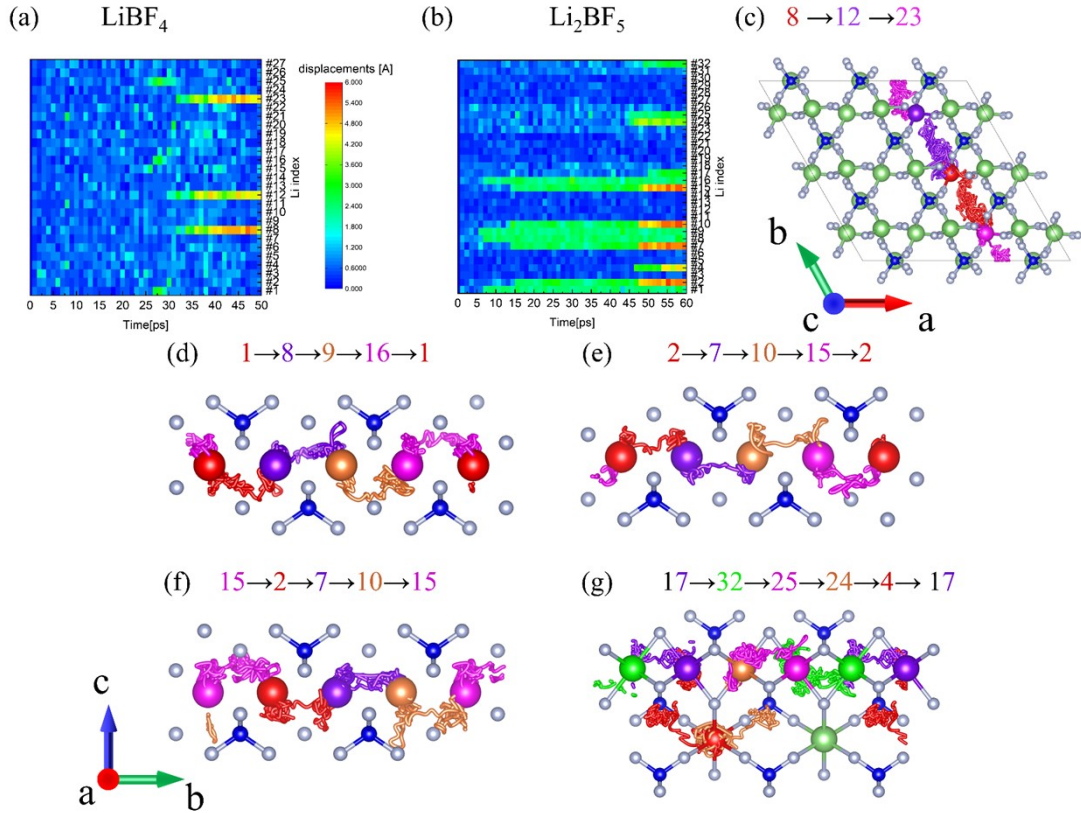


Figure S2. The displacement maps for each lithium ion in (a) LiBF_4 and (b) Li_2BF_5 respectively. (c) is the diffusion event in LiBF_4 during 30-40ps. (d)-(g) are four diffusion events in Li_2BF_5 during 5-8ps, during 13-15ps, during 45-49ps and during 44-55ps respectively. Except the 4th and 24th lithium ions in the fourth diffusion event diffusing across *ab* plane, other lithium ions diffuse along *ab* plane.

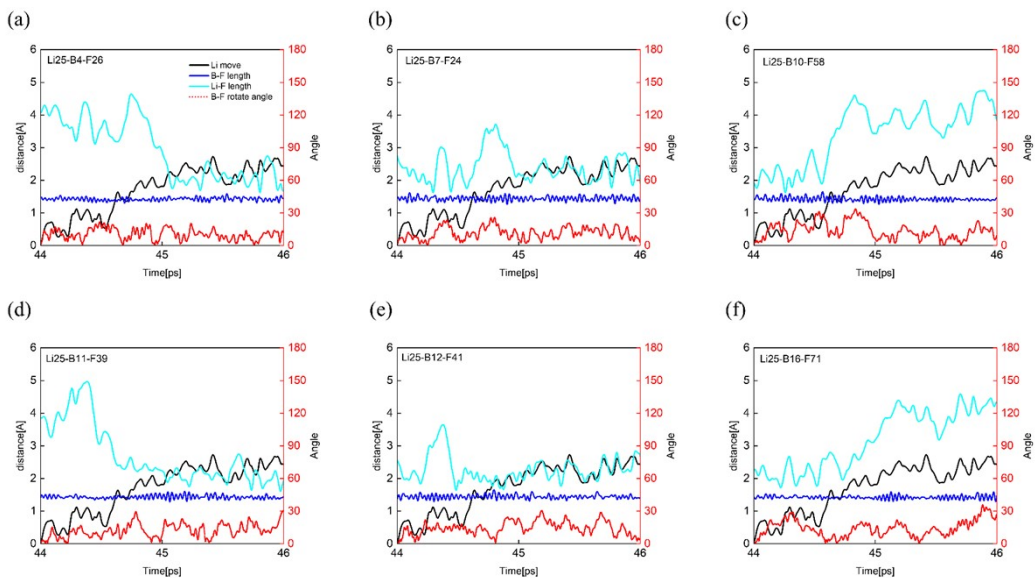


Figure S3. The displacements of the 25th Li^+ (the black solid line), the distance between the around B^{3+} and the F^- linked with it (the blue solid line), the distance between the 25th Li^+ and the F^- linked with the around B^{3+} (the cyan solid line) and

the angle change for the rotation of the B-F bond (the red dotted line) in Li_2BF_5 during 44-46ps.

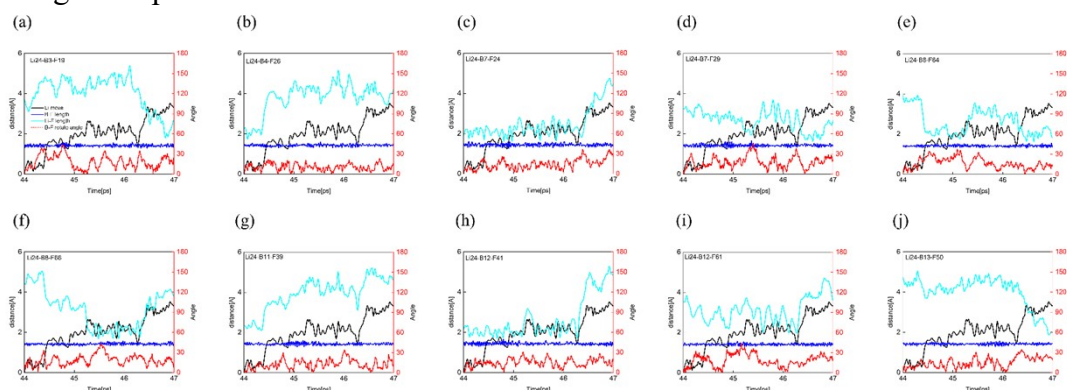


Figure S4. The displacements of the 24th Li^+ (the black solid line), the distance between the around B^{3+} and the F^- linked with it (the blue solid line), the distance between the 24th Li^+ and the F^- linked with the around B^{3+} (the cyan solid line) and the angle change for the rotation of the B-F bond (the red dotted line) in Li_2BF_5 during 44-47ps.

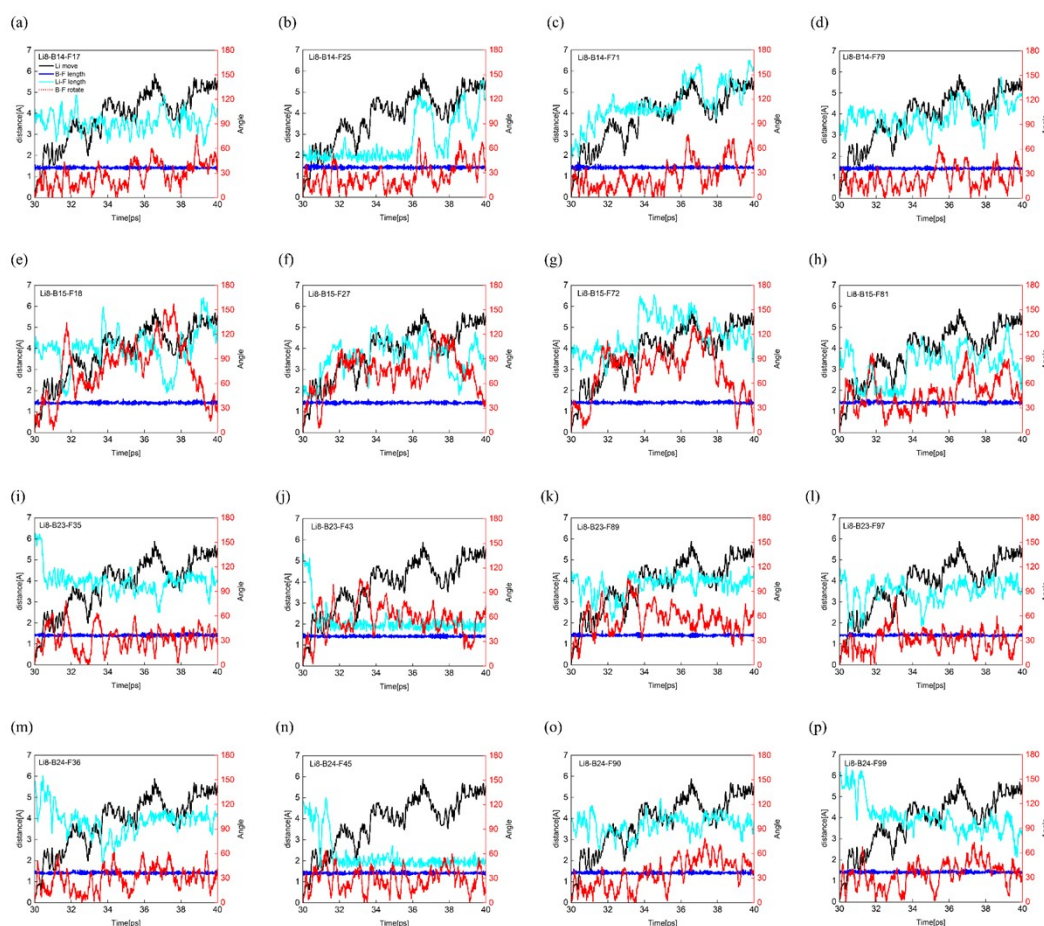


Figure S5. (a)-(p) are the displacements of the 8th Li^+ (the black solid line), the distance between the around B^{3+} and the F^- linked with B^{3+} (the blue solid line), the distance between the 8th Li^+ and the F^- linked with the around B^{3+} (the cyan solid

line) and the angle change for the rotation of the B-F bond (the red dotted line) in LiBF_4 during 30-40ps.

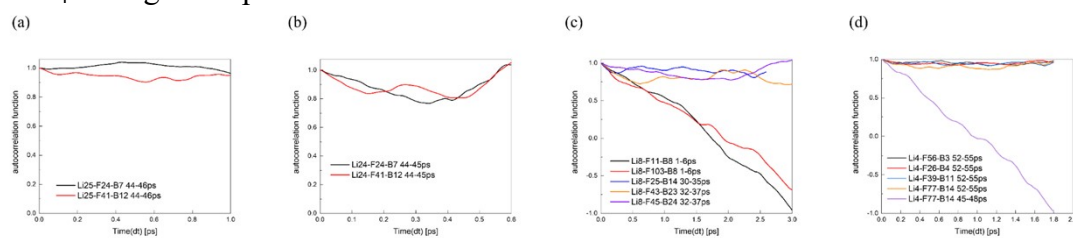


Figure S6. The autocorrelation function for (a) Li25 in Li_2BF_5 , (b) Li24 in Li_2BF_5 , (c) Li8 in LiBF_4 and (d) Li4 in Li_2BF_5 .

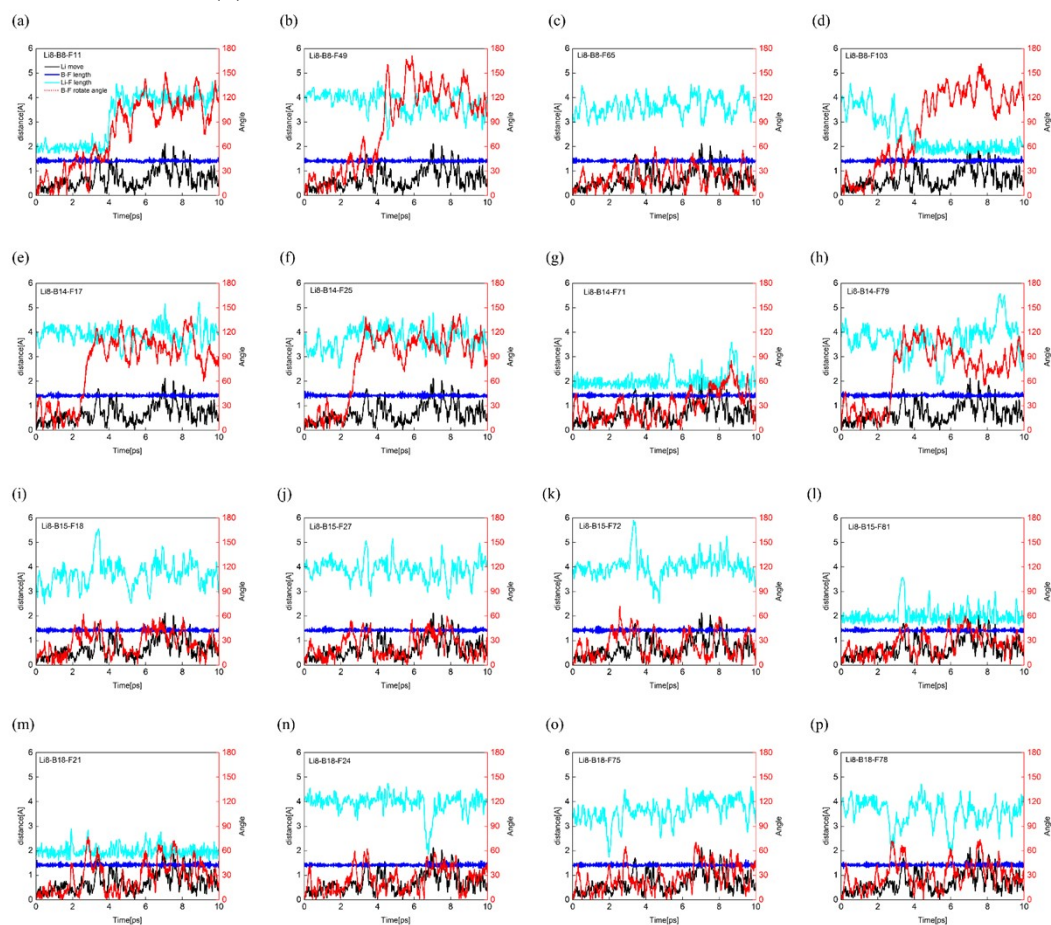


Figure S7. (a)-(p) The displacements of the 8th Li^+ (the black solid line), the distance between the around B^{3+} and the F^- linked with B^{3+} (the blue solid line), the distance between the 8th Li^+ and the F^- linked with the around B^{3+} (the cyan solid line) and the angle change for the rotation of the B-F bond (the red dotted line) in LiBF_4 during 0-10ps.

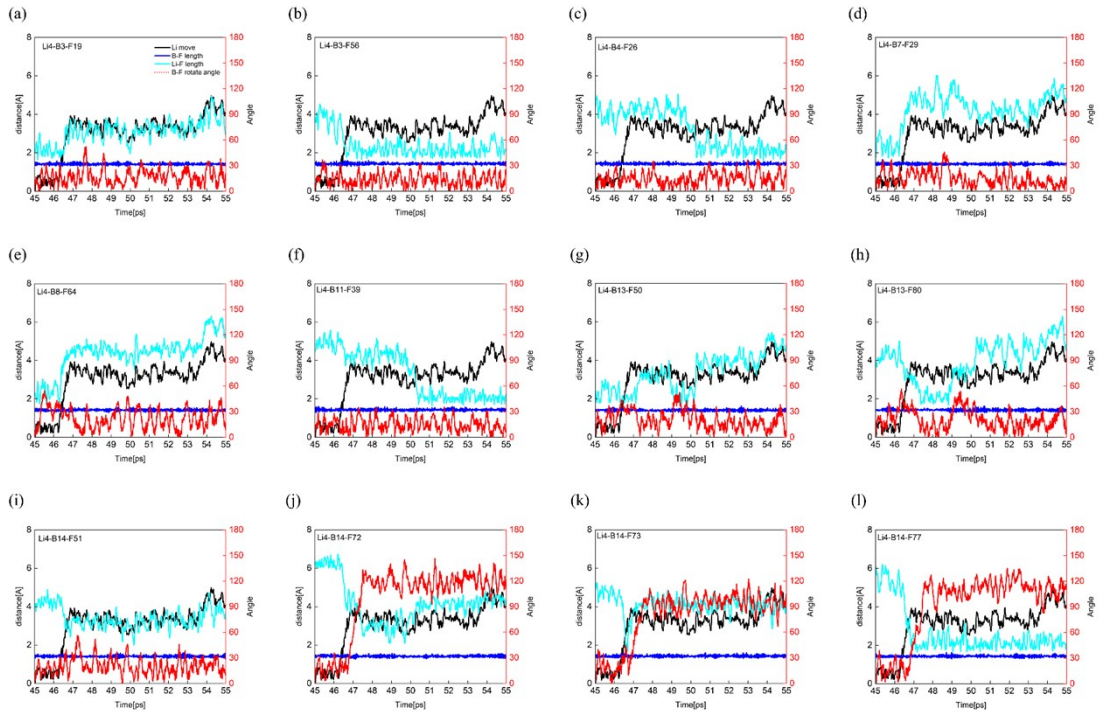


Figure S8. (a)-(l) The displacements of the 4th Li^+ (the black solid line), the distance between the around B^{3+} and the F^- linked with it (the blue solid line), the distance between the 4th Li^+ and the F^- linked with the around B^{3+} (the cyan solid line) and the angle change for the rotation of the B-F bond (the red dotted line) in Li_2BF_5 during 45-55ps.

Methods

The Bond-valence⁴⁴ simulation is the same as our previous work^{41,45}.

If the anions have formed a connected path in the same anion groups as a circle, we labeled it as ‘rotation’ and the minute energy to form it was labelled as E_{rot} . ‘Vibration’ was labelled as the energy less than E_{rot} . The example is shown in Figure. S9 and S^{2-} has formed the connected path in the same PS_4^{3-} so we labeled the minute energy to form it as E_{rot} in Figure. 1. Any situation whose energy is smaller than it is called ‘vibration’ while the situation whose energy is larger than it but smaller than E_{mig} is called ‘rotation’.

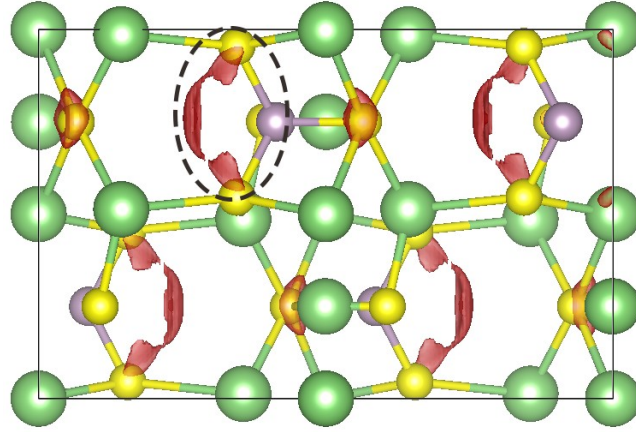


Figure S9 An example to show how to judge whether it is rotation and in black dotted circle the S^{2-} forms a connected path in the same PS_4^{3-}

AIMD simulation is used NVT ensemble⁴⁶ at 600K with a step of 1fs and only gamma point was considered and $LiBF_4$ was expand as $3 \times 3 \times 1$ while Li_2BF_5 was expand as $4 \times 4 \times 1$ to ensure larger than 10 \AA in supercells.

Calculation methods in Figure S3-8:

Black line: Li move distance was calculated as Equation S14 and t_{ini} represents the initial time while t represents time interval after t_{ini} .

$$|r(t)| = |x(t + t_{ini}) - x(t_{ini})| \quad (S14)$$

Blue line: B-F distance was calculated as Equation S15.

$$d_{B-F}(t_{ini} + t) = |x_B(t_{ini} + t) - x_F(t_{ini} + t)| \quad (S15)$$

Cyan line: Li-F distance was calculated as Equation S16 similar with S15.

$$d_{Li-F}(t_{ini} + t) = |x_{Li}(t_{ini} + t) - x_F(t_{ini} + t)| \quad (S16)$$

Red line: B-F rotation angle was calculated as Equation S17.

$$\theta_{B-F}(t + t_{ini}) = \arccos\left(\frac{r_{B-F}(t_{ini}) \cdot r_{B-F}(t_{ini} + t)}{|r_{B-F}(t_{ini})| \times |r_{B-F}(t_{ini} + t)|}\right) \quad (S17)$$

How to judge the rotation:

It is necessary to find out what could be viewed as rotation. Different people may have different standards. In Ref. 26, J. Smith et. Al takes $30-45^\circ$ as rotation and the same as in Ref. 24 and 27. Strictly speaking, in T_d symmetry, only larger than 120° as shown in Figure S10 with the changes from a-b-c to c-a-b (or 60° which climbs over the barrier) could be classified as rotation while less than 120° should be classified as vibration. Whether the former or the later, it can be confirmed that the large deviation must exist in the materials above 0K and may have an important effect on the diffusion of Li. As shown in Figure S11, with the temperature increases, it is easier to rotate with

a large angle which is the same as the diffusion of Li and more details in Figure S12 with atom probability distributions in $\text{LiBF}_4/\text{Li}_2\text{BF}_5$ during AIMD simulation. Rotation or not rotation is depended on the partition criterion and does not have any effect on the conclusion.

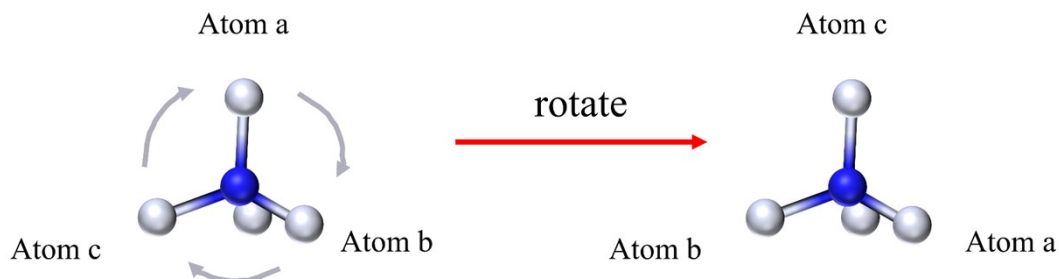


Figure S10. Rotation in AB_4 group with T_d symmetry.

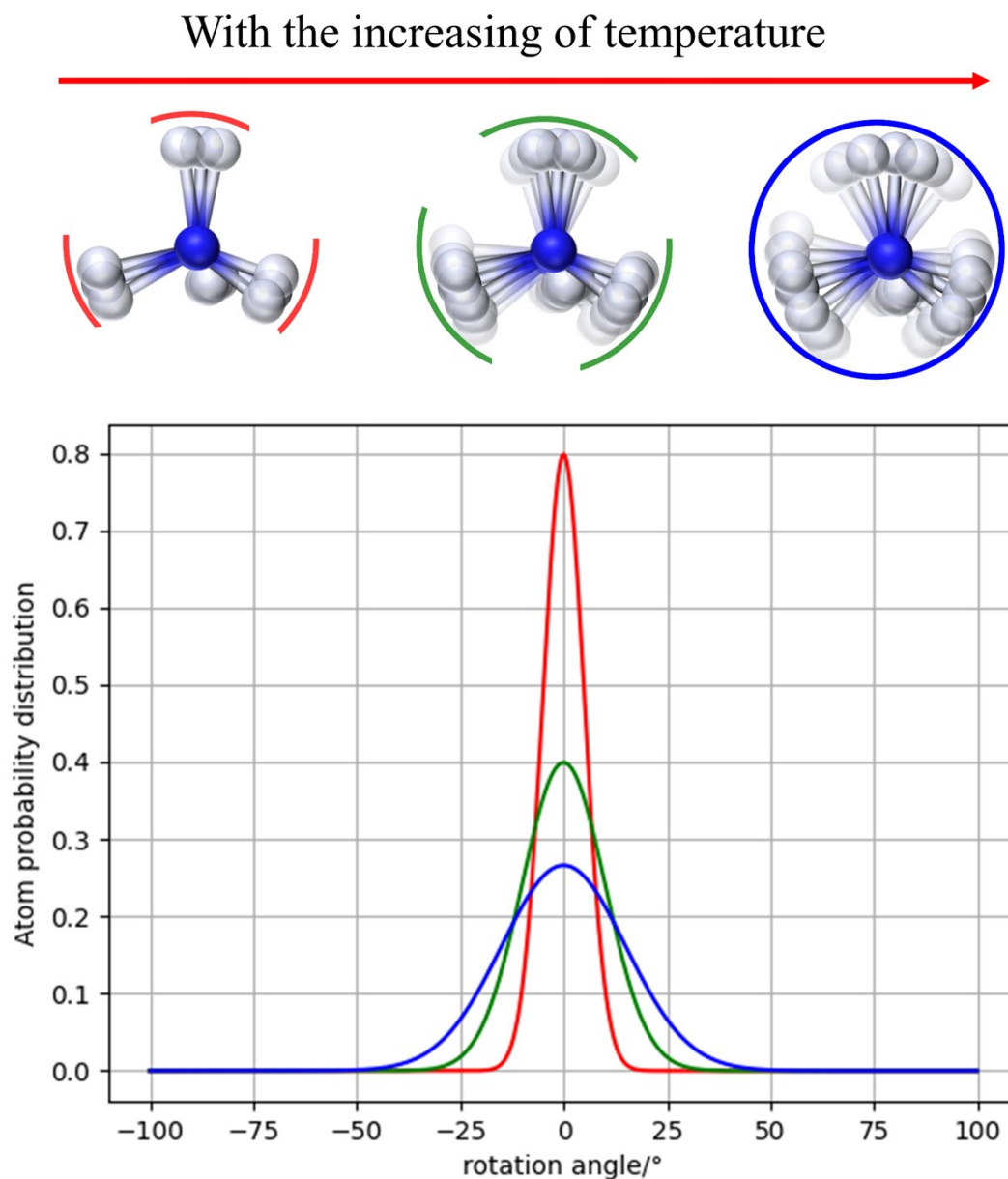


Figure S11. Supposing the rotation angle obeys the normal distribution (or any other distribution is the same). With the increasing of temperature, more chances for T_d group to rotate as larger angle even 120° (60° is OK because it rotates across the barrier).

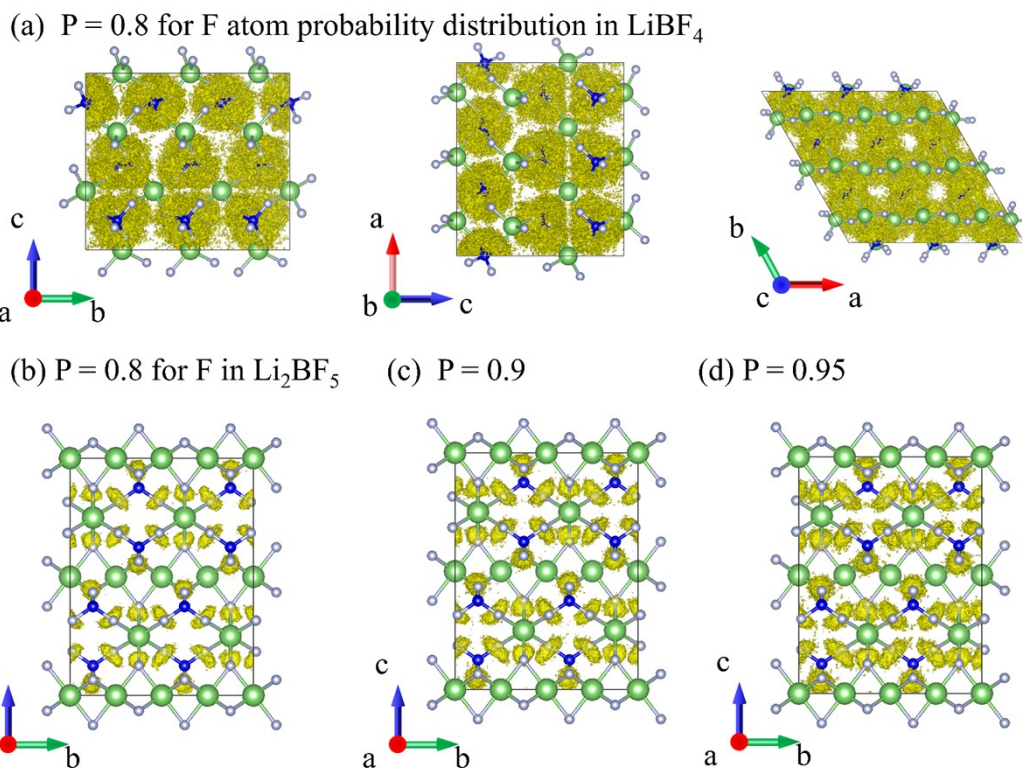


Figure S12 F probability distributions in $\text{LiBF}_4/\text{Li}_2\text{BF}_5$ during AIMD simulation. (a) F in LiBF_4 from the view of **a**, **b**, **c** axis with $p = 0.8$. (b)-(d) are F in Li_2BF_5 with $p = 0.8, 0.9, 0.95$ respectively.

In Methods we show how to judge in BV and it is easier because it has more sampling in space so we divide it as following: if the anions have formed a connected path in the same anion groups as a circle, we labeled it as ‘rotation’ and the minute energy to form it was labelled as E_{rot} . ‘Vibration’ was labelled as the energy less than E_{rot} .

However it is difficult to divide it in AIMD. In AIMD we judge it as rotation when the rotation angle during the diffusion of Li is larger than the average rotation angle because AIMD is based on statistics and time-dependent. It is more difficulty to do the same sampling as that in bond-valence because it is hard to sampling among all the space. Considering molecular dynamics is based on statistics and we have achieved enough time to make a statistic, we divide it whether has larger angle during the diffusion of Li than average angles. As shown in Figure S7(c) and (g), the diffusion of Li is accompanied by the rotation of BF_4^- (about 90° while the average is about 60°)

while as shown in Figure S5(b) in Li_2BF_5 there has no discrepancy so we labelled it as *vibrational*-type. But if we following the Ref .24, 26 and 27, we can both call them *rotational*-type.

What is coupling mechanism

From the intuition, coupling means the equal physical quantity e.g., time, space, frequency and energy as shown in Ref. 24. Considered the frequency of Li diffusion is about 10^{12} - 10^{13}s^{-1} (0.1ps-1ps), If we capture the signal longer than 1ps, it may present statistical significance rather the ‘couple’ in the strict sense. For example, if the frequency is 10^{12}s^{-1} , that means if the time sensitivity is larger than ps time level (cannot distinguish the details in smaller time level) or collection time is longer than 10ps (present statistical significance), we cannot identify the coupling. Unfortunately, we should capture the enough signal at longer time level due to the sensitivity of experiments. Here we present two figures to further illustrate it. The first one is the atom probability distribution in the supercell LiBF_4 and Li_2BF_5 as shown in Figure S12, obviously the F in Li_2BF_5 is more localization than that in LiBF_4 but we cannot deny the existence of rotation in BF_4^- in Li_2BF_5 as it shown in Figure S12(d). So if we extend the simulation time it may have more rotation events (not probability) for BF_4^- in Li_2BF_5 . It is the same as the neutron and other experiments which the longer time level and time-independent results may misjudge it. The second figure is based on the normal distribution in Figure S11 that larger rotate needs larger energy and it is more difficulty to appear (which is not equal to nonexistent and the same as the diffusion of Li and side effect). If we have enough time, we can also capture these events.

So in order to verify the coupling mechanism between Li^+ and BF_4^- we choose the lower simulation temperature (600K) and only focus on the diffusion process.